

FREQUENCY DEPENDENCE OF THE RESISTANCE AND INDUCTANCE OF SOLID CORE MAGNETS

Gustavo R. Gonzalez and Amedeo Brambilla*
Cambridge Electron Accelerator
Cambridge, Massachusetts

Abstract

A simple model is used to obtain, from basic field theory, expressions for the equivalent dynamic resistance and inductance of non-laminated iron core magnets when small amplitude sine waves modulate the D.C. magnet excitation. The approximations involved when applying the model equations to practical magnets are discussed. Deviation of calculated values from experimental data is of the order of 10% when the level of magnet excitation is low. Computed values of R and L may be used for field stability and ripple reduction studies.

1. Experiments Performed

Experiments were performed to measure R and L for different types of magnets. The magnets were excited at different D.C. levels using a current regulated power supply. The output of this supply was modulated with a low frequency sine wave using an oscillator in series with the power supply reference voltage (see Fig. 1).

Results show the basic difference between laminated and solid core magnets. The curves for the former indicate the characteristic behavior of a first order R-L circuit: (a) admittance decreasing at frequencies higher than a cut-off frequency, f_c , with an asymptotic slope of 20db/decade, and (b) phase shift approaching 90° for higher frequencies.

This is not the case for a typical solid core magnet (Fig. 2). The admittance curves have a slope of much less than 20db/decade at high frequencies. At any given frequency the admittance is less for lower D.C. excitation. The phase curves never reach 90° and show an oscillatory behavior with an absolute minimum which is lower for lower values of D.C. excitation. The phase curves cross over as the frequency is increased and reverse their order with small angles exhibited for small D.C. excitation. They seem to have a high frequency asymptote of 50 to 70°.

* 1) A. Brambilla is now at Yale University.

2) This work was supported by the Atomic Energy Commission.

Figure 3 clearly shows that the curves for the unsaturated solid iron magnets may be normalized to a universal curve, indicating there are common features among magnets of different geometries. The curves were arbitrarily normalized by shifting them, using the ratio f/f_r , where f_r is a magnet characteristic frequency.

2. Theoretical Model

In theory it is possible to calculate an equivalent magnet resistance from the total energy losses, and a magnet inductance from the total energy stored in the magnetic field. In order to do that the fields must be known at every point, implying a solution of the Maxwell or potential equations subject to the required boundary conditions. This is a difficult task because: (1) each magnet has a complex geometry, and (2) the presence of the iron introduces non-linearities in the equations.

Nevertheless, the fact that the admittance curves may be normalized to universal curves leads us to believe that a model of simple geometry should exist for a wide range of magnets. This model would exhibit the same general trends of the magnets and would allow us to predict, approximately, the dynamic response of real magnets.

The mathematical model chosen is a magnet of rectangular cross section, extending to infinity in the y and z direction as indicated in Fig. 4. Two dimensions characterize the model, the dimension of the pole face in the "x" direction, "d", and the height of the gap, "g".

The solution of Maxwell equations in iron is well known. The only modification introduced is that we used the reversible permeability¹ of iron instead of the normal permeability. The reason is that we are interested in the response of the magnet when excited by a sinusoidal current superimposed on a constant current.

The calculation of the field in the air is simplified by solving the quasi-static problem using the scalar potential.

This is justified because, at the low frequencies involved, the fields have practically the same phase in the neighborhood of the gap. The Laplace equation is solved from simplified boundary conditions obtained from the solution of Maxwell equations in the iron. This is not rigorous but it seems the simplest approximation. The usual assumption that the iron surfaces are equipotential, used for D.C. calculations, breaks down because the high frequency fields concentrate near the corners and the magnetic potential difference across the gap is much smaller at the point $x = 0$, than at the points $x = \pm d/2$.

The losses in the iron consist of: (1) those produced by the eddy currents in the iron which may be calculated from the solution of Maxwell equations neglecting end effect due to the gap, and (2) those produced by hysteresis while the fields trace a minor loop in the B-H graph. The hysteresis losses per unit volume may be assumed to be proportional to $(\Delta B)^2$ and thus may be calculated as the eddy current losses.

In order to integrate the losses over all the iron volume we must not have an infinite magnet, and we have to assign specific values for the magnet dimensions in the z and y directions.

The losses in the copper conductor are assumed equal to the D.C. losses. Since the measured increase in resistance for laminated magnets is small compared with the increase for solid magnets, we expect that the increase in copper losses, due to skin effect, is small compared with the iron losses.

The energy stored consists of: (1) that stored in the iron, which may be calculated from the solution of Maxwell equations neglecting end effects due to the gap, and (2) that stored in the air, which may be calculated from the solution of the scalar potential equation in the gap.

3. Theoretical Equations

Using the described model, we obtain after long calculations:

$$R = R_c + \frac{2w\ell\eta N^2}{\delta\mu^2 \left(\frac{\ell}{\mu} + \frac{4g}{8 + \frac{3\pi g}{\delta}}\right)^2} \times$$

$$\frac{(\sinh \frac{d}{\delta} - \sin \frac{d}{\delta}) + 4\mu\eta(\sinh \frac{d}{\delta} + \sin \frac{d}{\delta})}{(\cosh \frac{d}{\delta} + \cos \frac{d}{\delta})} \quad (1)$$

$$L = \frac{4\pi N^2 w\delta \left(\frac{\ell}{\mu} + g\right)}{10^9 g \left(\frac{\ell}{\mu} + \frac{4g}{8 + \frac{3\pi g}{\delta}}\right)} \times$$

$$\frac{\sinh \frac{d}{\delta} + \sin \frac{d}{\delta}}{\cosh \frac{d}{\delta} + \cos \frac{d}{\delta}} \quad (2)$$

where

d	=	Dimension of magnet pole
f	=	Frequency
g	=	Gap dimension
ℓ	=	Length of path of integration in the magnet
N	=	Number of turns in two poles
R _c	=	Coil resistance
w	=	Length of magnet
δ	=	Skin depth = $\sqrt{2\pi f\mu\sigma}$
η	=	Steinmetz hysteresis coefficient
μ	=	Differential permeability
ρ	=	Resistivity

These expressions include a factor composed of hyperbolic and circular functions of the dimensionless parameters d/δ . The origin of this factor is the field distribution in the iron, due to eddy currents. There is also another factor in which the dimensionless parameter g/δ appears. This factor comes from the application of Ampere's Law, and represents the reluctance of the magnetic circuit.

Asymptotic expressions may be obtained for low frequencies when $\delta \gg d, g$, and for higher frequencies when $\delta \ll d, g$, (until the model analogy breaks down). At high frequencies the time constant $\tau = L/R$, varies inversely with the frequency.

4. Application To Magnet Calculations

In practice, the magnet parameters d, g, w, ℓ , may not have a precisely defined value as in our model because of the different geometries of magnets. Judgment must be exercised in assigning values to these parameters.

1. For magnets of more than one pair of poles, a multiplying factor equal to the number of pairs of poles must be applied to both R and L.

2. For magnets of type C, an effective ℓ must be used (Fig. 4).

3. For magnets of type H, since the alternating field is pushed to the surfaces, the volume over which there is

appreciable field is about twice that of a magnet of type C. One way to compensate for this effect would be to consider that this type of magnet is equivalent to two magnets of type C with $d' = d/2$.

4. Rather than using the parameters d , l , w , it may be possible to use the area of iron surface (S), and the area (A), and perimeter (p) of the pole face. This seems logical since at low frequencies the field covers the whole cross sectional area, and at high frequencies the field is concentrated in a strip of width (δ) along the perimeter. Characteristic distances may be defined as $d' = 2A/p$; $w' = p/2$; $l' = S/p$; which, for long magnets, reduce to d , w , and l .

5. Also since d has not a definite value there is not a definite cut-off frequency for L , but rather a combination of a large number of cut-off frequencies. Under this condition the cut-off is not as sharp, and we may approximate:

$$\frac{\sinh d/\delta + \sin d/\delta}{\cosh d/\delta + \cos d/\delta} \approx \tanh d/\delta$$

5. Results

The low frequency asymptotic expression for L provides one way of calculating μ from experimental results of one magnet if we know the geometrical parameters w' , d' , l' , g' , and the number of turns, N , of the tested magnet. Similarly the other asymptotic expression for L provides a way of calculating ρ , once we know μ . The Steinmetz coefficient may then be calculated from the high frequency asymptotic expression for R .

We should expect to obtain a very low value for the reversible permeability, μ , compared with the normal permeability. Values published by Bozarth² indicate that $25 < \mu < 60$. Published values for the other iron parameters are: $10 \times 10^{-6} \Omega \text{cm} < \rho < 60 \times 10^{-6} \Omega \text{cm}$ for the resistivity, ρ , and $.0004 < N < .002$ for the Steinmetz hysteresis coefficient.^{4, 5}

Calculations were made only for low values of D.C. so that the magnet is far from saturation. Then it was expected that the calculated set of μ , ρ , η , would approximate the experimental values of the other three magnets. Results from the experimental data for the 3-inch clearing magnet (Fig. 5) gives the following set of values: $\mu = 35$; $\rho = 70 \times 10^{-6} \Omega \text{cm}$; $\eta = .0018$. Using this set, calculations were made with the theoretical equations 1 and 2. The results shown in Figures 5 to 8

indicate the same trends as the experimental data. Deviation between theoretical and experimental values are of the order of 10%.

6. Discussion of Results

Figure 8 shows the result for a bubble chamber magnet which has a very complicated shape, much different than our model. Nevertheless, the deviation of experimental data from the theoretical values is not great. In this case it is apparent that the deviation follows an oscillating pattern. A similar pattern, but of smaller amplitude, can be found in the experimental data for the other three magnets. A possible explanation is that the geometrical parameter d' has not a definite value, as assumed in our theory. Then the R and L would be obtained from a summation of similar terms, each with a different d' , as required from the magnet shape. Obviously, each term in the summation would have a different cut-off frequency, and the curves would appear to have an oscillatory pattern. The approximation in the previous comment, Section 4-5, gives the average of these oscillations.

A common feature of the phase plots is the asymptotic behavior at high frequencies. From the equations it is seen that if for some magnets

$$\frac{1 + l/\mu g}{1 + 4 \mu n} \approx 1$$

then the phase approaches 45° . The deviation from this for any magnet is determined by the ratio l/g .

The high value of the resistivity used can be traced back, in part, to the simplified boundary condition assumed to hold between the iron pole and air gap.

At high excitation the permeability is reduced, and the relative value of the energy stored in the iron increases as compared with that stored in the gap. This increases the importance of the iron shape, and a new model must be used in the analysis. Nevertheless, general trends may be predicted from the low excitation analysis using the asymptotic expressions:

1. The low frequency inductance should decrease since μ is reduced.

2. Since the iron, as mentioned before, is of greater importance, the dimension d' should be increased because normally the iron cross section is larger than the gap cross section. This implies that the inductance cut-off frequency

determined by the ratio d'/δ , will be smaller than expected, and the high frequency inductance also decreases.

3. The low frequency resistance does not change.

4. The high frequency resistance is reduced by a reduction in μ .

5. Also the fact that the time constant is decreased at low frequencies, and increased at high frequencies, implies that the phase plots corresponding to two different D.C. excitation levels must cross each other.

All these predictions are confirmed by experimental data (Fig. 2).

7. Conclusions

The proposed model can be used, for low excitation currents, to calculate the magnet equivalent dynamic resistance and inductance with an accuracy of the order of 10% up to a frequency of 500 cps. It can also be used to predict the general trends of R and L as the excitation current is increased. The deviation of theoretical results from experimental data is due to the simplifications made.

Then we conclude that the behavior of non-laminated iron core magnets, as the exciting current frequency increases up to 500 cps, is explained by the penetration of fields in the iron core and is independent, up to a first approximation, of the field penetration in the copper conductors.

At higher frequencies, as the skin depth approaches zero, the fields are driven out of the iron core and we should expect that leakage flux and copper conductors play a more important role.

For the types of iron normally used for D.C. electro-magnets (low carbon steel) the set of values μ, ρ, η , should not differ much, and the set given in this report may be used. It should be remembered that ρ is an effective resistance; higher than the one normally found in tables.

Then the procedure for calculating the low excitation R and L for a magnet is as follows:

1. Determine the equivalence of the magnet in terms of a number of type C magnets as indicated in Section 4-1, 4-2, and 4-3.

2. Determine the effective values of d, g, w, ℓ, N , for the equivalent type C magnets as indicated in Section 4-4.

3. Calculate the R and L for the equivalent C magnets from formulas 1 and 2 as indicated in Section 4-5.

4. Calculate the R and L of the magnet from steps 1 and 3.

References

1. Pender H. and William Del Mar, Electrical Engineers' Handbook, Fourth Edition pp. 2-86, New York, N.Y. John Wiley & Sons.
2. Bozarth, R.M., Ferromagnetism, New York, N.Y., D. Van Nostrand Co., 1951, p. 58, Fig. 3-7.
3. Pender H. and William Del Mar, Electrical Engineers' Handbook, Fourth Edition pp. 2-89, New York, N.Y. John Wiley & Sons.
4. Pender H. and William Del Mar, Electrical Engineers' Handbook, Fourth Edition pp. 2-89, New York, N.Y. John Wiley & Sons.
5. Bozarth, R.M., Ferromagnetism, New York, N.Y., D. Van Nostrand Co., 1951, p. 513, Table 5.

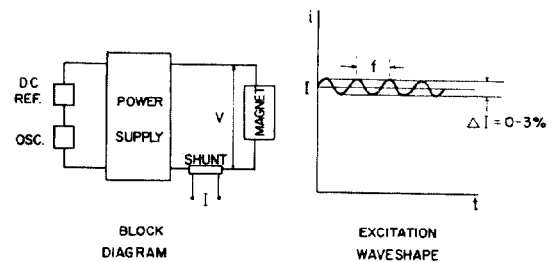


Figure 1.

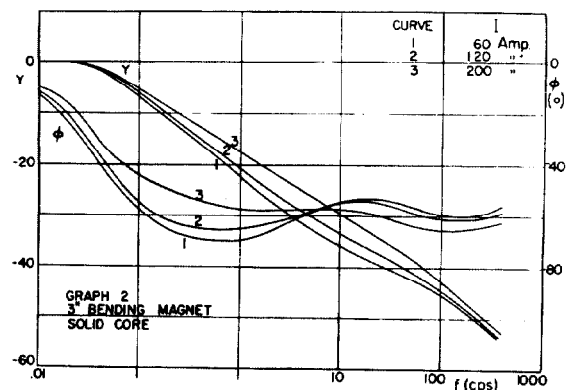


Figure 2.

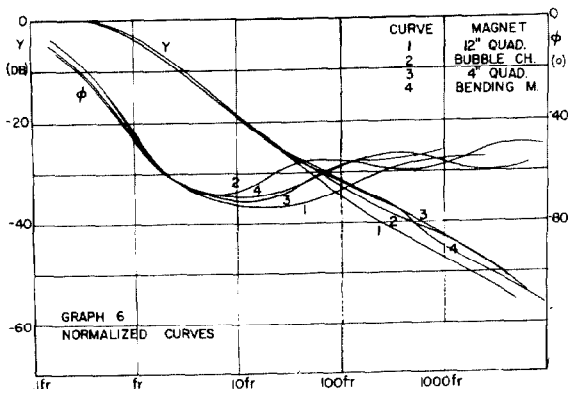


Figure 3.

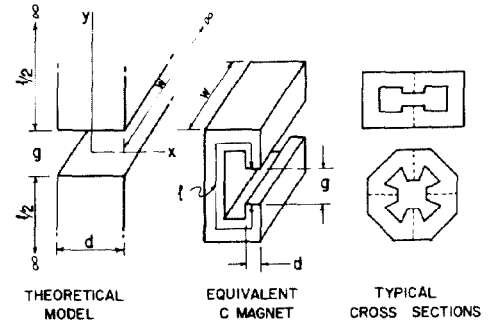


Figure 4.

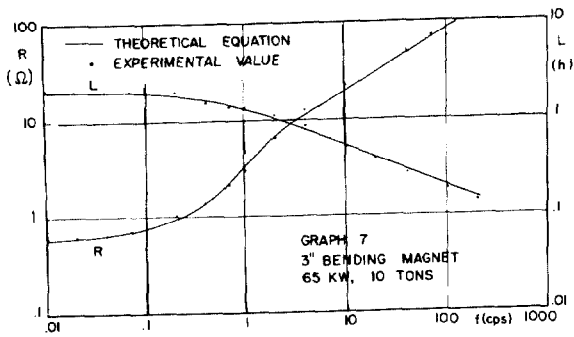


Figure 5.

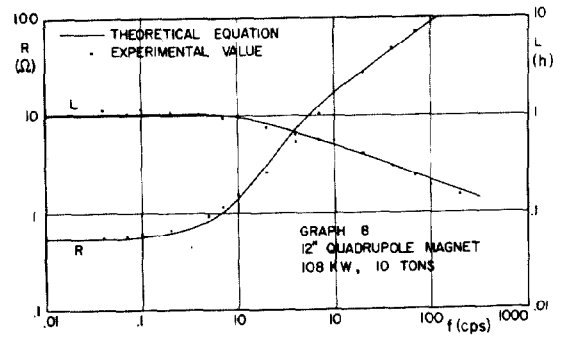


Figure 6.

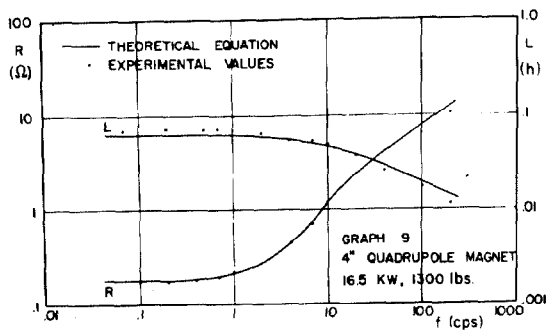


Figure 7.

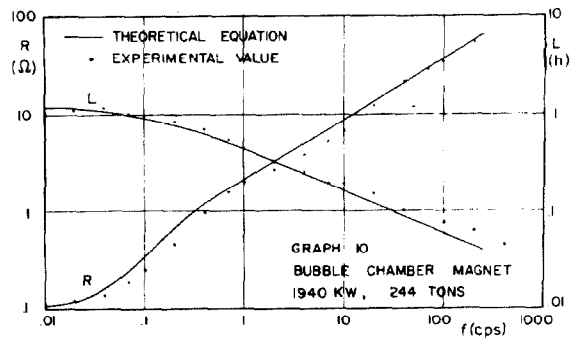


Figure 8.